Identification of a Reactive Metabolite of Terbinafine: Insights into Terbinafine-Induced Hepatotoxicity

Suzanne L. Iverson[†] and Jack P. Uetrecht*[,†,‡]

Faculties of Pharmacy and Medicine, University of Toronto, Toronto, Ontario, Canada

Received September 13, 2000

Oral terbinafine treatment for superficial fungal infections of toe and fingernails is associated with a low incidence (1:45000) of hepatobiliary dysfunction. Due to the rare and unpredictable nature of this adverse drug reaction, the mechanism of toxicity has been hypothesized to be either an uncommon immunological or metabolically mediated effect. However, there is little evidence to support either mechanism, and toxic metabolites of terbinafine have not been identified. We incubated terbinafine with both rat and human liver microsomal protein in the presence of GSH and were able to trap an allylic aldehyde, 7,7-dimethylhept-2-ene-4-ynal (TBF-A), which corresponds to the N-dealkylation product of terbinafine. TBF-A was also prepared synthetically and reacted with excess GSH to yield conjugates with HPLC retention times and mass spectra identical to those generated in the microsomal incubations. The major GSH conjugate, characterized by ^{1}H NMR, corresponds to addition of GSH in a 1,6-Michael fashion. There remains a second electrophilic site on this metabolite, which can bind either to a second molecule of GSH or to cellular proteins via a 1,4-Michael addition mechanism. Moreover, we demonstrated that the formation of the GSH conjugates was reversible. We speculate that this allylic aldehyde metabolite, formed by liver enzymes and conjugated with GSH, would be transported across the canalicular membrane of hepatocytes and concentrated in the bile. The mono-GSH conjugate, which is still reactive, could bind to hepatobiliary proteins and lead to direct toxicity. Alternatively, it could modify canalicular proteins and lead to an immune-mediated reaction causing cholestatic dysfunction.

Introduction

Terbinafine (Lamisil, Figure 1) represents a new class of antifungal agents used for the treatment of superficial fungal infections of the toe and fingernails (*1*, *2*). The oral formulation has been on the market in various countries for more than eight years, and as of 1997, more than 7.5 million individuals had been treated with this drug (*3*). Terbinafine revolutionized the treatment of superficial fungal infections because it concentrates in keratin-rich tissues, and it is fungicidal as opposed to fungistatic. The drug selectively inhibits fungal squalene epoxidase, and it is thought that this increases the extracellular concentration of squalene to toxic levels, thus killing the fungal cell (*2*).

There are several adverse drug reactions associated with the use of oral terbinafine (*4*, *5*). A postmarketing surveillance study of more than 25 000 patients showed that mild to severe gastrointestinal, skin, and taste disturbances are the most common adverse events related to oral terbinafine treatment (*6*). Hepatobiliary dysfunction is a rare adverse drug reaction of TBF. Such cases are usually asymptomatic and reversible; however, symptomatic cholestatic injury occurs in 1 of 45000−54000 exposed patients (*7*).

Cholestasis results when hepatocellular bile secretion is impaired. Alterations of bile secretion by the hepatocyte, or hepatocellular cholestasis, can occur either with hepatocellular damage (i.e., "mixed" or "hepatitis"), as in the case of terbinafine-induced cholestatic hepatitis, or without damage to hepatocytes (i.e., "pure"), as in the case of estrogen-induced cholestasis (*8*). Obstruction can also occur in extrahepatic bile ducts (sclerosing cholangitis) or intrahepatically when either ductules (cholangiolitis) or interlobular ducts (cholangitis) are obstructed. The terbinafine case studies outlined in the discussion below describe varying severities of enzyme level elevation coupled with increased cholesterol and bilirubin levels, which are clinically indicative of mixed cholestatic hepatitis and cholangiolitis/cholangitis.

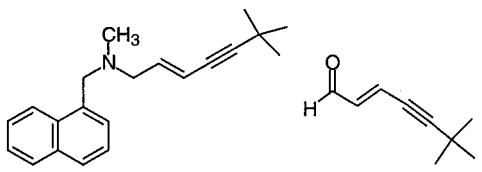

Terbinafine **TBF-A**

Figure 1. Chemical structures of terbinafine and TBF-A.

The pathogenesis of drug-induced bile duct injury remains, for the most part, unknown. Yet there exist a few animal models that indicate reactive metabolites of the disease-causing drug are a common pathogenic feature (*9*, *10*). Fifteen hepatic metabolites of terbinafine were identified during preclinical and clinical trials in the late 1980s, yet none were considered reactive enough, or too reactive, to mediate an adverse drug reaction (*11*−*13*). The major routes of biotransformation that were

* To whom correspondence should be addressed: Faculty of Pharmacy, University of Toronto, Toronto, Ontario, Canada M5S 2S2. Telephone: (416) 978-8939. E-mail: jack.uetrecht@utoronto.ca.
† Faculty of Pharmacy.
‡ Faculty of Medicine.

10.1021/tx0002029 CCC: $20.00 © 2001 American Chemical Society
Published on Web 01/16/2001

discovered included oxidation of the naphthalene moiety, N-dealkylation, and aliphatic oxidation of the *tert*-butyl group.

Terbinafine undergoes nonselective aromatic oxidation of the naphthalene ring system to yield dihydrodiols, for which arene oxides are the presumed intermediates, but no naphthols, mercapturic acids, or other products were identified. Epoxides (arene oxides) have long been considered to be reactive metabolites responsible for adverse drug reactions (*14*). This pathway was considered to be a detoxification step since the dihydrodiol was reported to be glucuronidated and excreted (*11*).

Another potentially harmful metabolic pathway, described in the same publication (*11*, *12*), involves N-dealkylation at the allylic N−C bond which likely yields an allylic, propargylic aldehyde (TBF-A,[1] Figure 1). This metabolite was not directly observed, presumably due to its reactivity, and it was suggested that the aldehyde probably undergoes oxidation to its corresponding carboxylic acid and is excreted, thus exerting no toxic effects on the host. We revisited this metabolic pathway to investigate the possible role of TBF-A in terbinafine-induced hepatobiliary dysfunction.

Materials and Methods

Materials. Terbinafine (Lamisil) and the TBF-A precursor [(*E*/*Z*)-1-bromo-7,7-dimethylhept-2-ene-4-yne (allyl-Br)] were generous gifts from Sandoz (now Novartis, Basel, Switzerland). Human liver microsomes were kindly provided by T. Inaba (Department of Pharmacology, University of Toronto, Toronto, ON). The microsomes were assayed and had relatively high levels of P450 2C9, 2D6, and 3A4. Pyridinium dichromate (98%), reduced GSH, and *N*-acetylcysteine (NAC) were obtained from Sigma-Aldrich Fine Chemicals (St. Louis, MO). All other chemicals and solvents were purchased from Sigma-Aldrich or Fisher Scientific (Toronto, ON) unless otherwise stated. All solvents used for HPLC analyses were HPLC grade.

Analytical. All ^{1}H NMR spectra were obtained with a Varian Unity-500 spectrometer (Palo Alto, CA) at 500 MHz. The LC portion of the LC/MS and LC/MS/MS experiments was performed using a LKB system (two LKB 2150 pumps with a LKB 2152 LC controller) and a Rheodyne injector (Cotati, CA). The liquid chromatograph was interfaced with a Sciex API III triple-quadrupole mass spectrometer (Perkin-Elmer Sciex, Thornhill, ON) equipped with an IonSpray interface. Collision-induced dissociation of selected precursor ions was performed in the RF-only quadrupole region, and argon was used as the target gas (1×10^{15} atoms/cm^3). The chromatography column consisted of a 5 μm packing of Ultracarb 5 ODS 30 (2 mm × 100 mm, Phenomenex, Torrance, CA). The gradient mobile phase initially consisted of 5% methanol in an aqueous solution (v/v) of 1% acetic acid and 2 mM ammonium acetate. This was increased to 35% methanol over the course of 2 min, allowed to remain isocratic for 15 min, then increased to 60% methanol over the course of 5 min, made isocratic for 10 min, and finally returned to the initial conditions over the course of 1 min. The flow rate of the HPLC solvent was 0.2 mL/min.

Rat liver microsomal incubations were analyzed by selective ion monitoring (SIM) where specific *m*/*z* signals corresponding to the GSH adducts and the parent compound were programmed for detection by the LC/MS system. LC/MS/MS experiments of the rat microsomal incubations were carried out with 100 μL injections. All human liver microsomal incubations (20 μL injections) were analyzed by multiple-reaction monitoring (MRM) where LC/MS and MS/MS analyses are conducted simultaneously. Q1 was set for parent ions *m*/*z* 292 and 444, and Q3 was set for their corresponding unique fragments with *m*/*z* values of 141 and 137. Reaction products other than TBF-A−SG adducts and the parent terbinafine were therefore not detected in either the SIM or MRM mode.

(*E*/*Z*)-7,7-Dimethylhept-2-ene-4-ynol. Briefly, 670 mg (600 μL, ρ = 1.1145 g/mL) of the allyl bromide [(*E*/*Z*)-1-bromo-7,7-dimethylhept-2-ene-4-yne] was added with stirring to 75 mL of 0.37 M sodium hydroxide in a 65% acetonitrile solution prepared in distilled, deionized water (>18.0 MΩ/cm). Drops of water were added as necessary to maintain solubility. The progress of the reaction was followed by TLC (100% ethyl acetate) where the R_f of the allylbromide was 0.73 and that of the alcohol was 0.60. The reaction proceeded with stirring for 24 h at room temperature, and then the acetonitrile was removed under vacuum to yield a yellow, cloudy, aqueous solution. Products were extracted with 3 × 20 mL portions of chloroform, dried with anhydrous magnesium sulfate, and concentrated by vacuum to a volume of 5 mL, which yielded a bright yellow viscous liquid. The alcohol was purified by reversed-phase TLC ($LKC_{18}F$, Whatman) using a mobile phase containing 65% methanol, 1% acetic acid, and 2 mM ammonium acetate in distilled, deionized water. The R_f of the bromide was 0.07, and that of the alcohol was 0.65. The alcohol band was removed and washed with water, eluted with methanol, evaporated to dryness under a stream of nitrogen, reconstituted in water, and then extracted into ethyl acetate. The ethyl acetate fraction was dried with anhydrous magnesium sulfate, filtered, and then concentrated to yield the allylic alcohol, which was determined by ^{1}H NMR to be 85% *E* isomer: ^{1}H NMR (CD_3OD) δ 1.20 (9H, s, t-Bu), 4.08 (2H, dd, J = 2.0 and 3.4 Hz, *E*-H1), 4.89 (s, OH exchange), 5.65 (1H, dt, J = 2.0 and 16 Hz, *E*-H3), 6.01 (1H, dt, J = 5.5 and 16 Hz, *E*-H2).

(*E*/*Z*)-7,7-Dimethylhept-2-ene-4-ynal (TBF-A). The allyl alcohol from the reaction described above (50.6 mg in 0.5 mL of methylene chloride) was added to a suspension of 0.20 g of pyridinium dichromate in 0.5 mL of methylene chloride (1.5 molar equiv). The reaction mixture was concentrated under a stream of nitrogen to a volume of 0.5 mL. The reaction vial was capped and wrapped in aluminum foil, while the contents were stirred overnight. Next, the mixture was diluted with 5 mL of methylene chloride. The product was filtered by gravity through a medium pore filter paper, and then through a fine pore filter paper, and rinsed several times at each stage with 1 mL aliquots of methylene chloride. The total dilution of the reaction mixture was 80-fold (40 mL). The liquor was concentrated under a stream of nitrogen to yield a brown liquid product. The product was purified on a small silica gel column (50 mg of silica loaded into a Pasteur pipet) and eluted with ethyl acetate. Purity was established by TLC (ethyl acetate) where the R_f of TBF-A was 0.70 and the isomeric purity was 85% *E* as determined by ^{1}H NMR (Figure 3A): ^{1}H NMR ($CDCl_3$) δ 1.30 (9H, s, t-Bu), 6.38 (1H, dd, J = 16.0 and 8.0 Hz, H2), 6.61 (1H, d, J = 16 Hz, H3), 9.53 (1H, d, J = 7.8 Hz, H1).

Reaction of TBF-A with GSH. A concentrated solution of TBF-A (7.62 mg in 0.1 mL of methylene chloride) was added dropwise to 50 mL of a 10 mM solution of GSH in 100 mM phosphate buffer (pH 8.0). The contents were sonicated for 2 min, and the reaction proceeded for 2 h, after which the reactants were concentrated under reduced pressure to approximately $^1/_3$ of the original volume. The GSH conjugates were extracted via a semipreparative C-18 cartridge (Chromatographic Specialties, Brockville, ON) using 10% acetonitrile as the eluent. The 10% acetonitrile fractions were concentrated by vacuum, leaving a bright yellow liquid, which was subsequently analyzed by LC/MS. For LC/MS analysis, approximately 0.5 mg was diluted in 0.1 mL of water. The flask containing the GSH adducts was dried with a lyophilizer for 3 h to remove traces of water prior to ^{1}H NMR analysis: ^{1}H NMR for the major adduct (D_2O) δ 0.8 (9H, m, t-Bu), 1.6 (2H, m, Gluβ), 2.05 (2H, m, Gluγ), 2.60 (1H, m, Cysβ), 3.25 (2H, m, Glyα), 4.05 (1H, m, Gluα), 5.90

[1] Abbreviations: TBF-A, 7,7-dimethylhept-2-ene-4-ynal; allyl-Br, (*E*/*Z*)-1-bromo-7,7-dimethylhept-2-ene-4-yne; NAC, *N*-acetylcysteine; SIM, selective ion monitoring; MRM, mulitiple-reaction monitoring; TBF-A−SG, 5-glutathionyl-7,7-dimethylhept-2,4-enal or 3-glutathionyl-7,7-dimethylhept-4-ynal; ANIT, α-naphthylisothiocyanate.

(1H, dd, J = 8.8 and 15.9 Hz, H2), 6.45 (1H, d, J = 11.5 Hz, H4), 7.40 (1H, dd, J = 11.4 and 15.9 Hz, H3), 9.05 (1H, d, J = 8.6 Hz, H1). The positive ion LC/MS spectrum consisted of peaks with retention times of 20 (minor adduct) and 22 min (major adduct), both having M + 1 ions at *m*/*z* 444 (100% relative intensity) and M + Na^+ ions at *m*/*z* 466 (50% relative intensity). The positive ion LC/MS/MS spectrum of the peak with a retention time of 22 min consisted of peaks at *m*/*z* 444 (30% relative intensity, TBF-A + GSH + 1) and 137 (100% relative intensity, TBF-A^+).

Reversibility of the Thiol Addition to TBF-A. A concentrated solution of TBF-A (5 mg in 200 μL of acetonitrile) was added dropwise with stirring to 85 mL of NAC [11 mM in 100 mM phosphate buffer (pH 8.0)]. The reaction proceeded for 3.5 h at ~60 °C, and the progress was followed by HPLC. The reaction was considered complete when no TBF-A was detected by HPLC. Approximately 2 mL was removed for LC/MS and LC/MS/MS analyses. The positive ion LC/MS spectrum of the NAC conjugates revealed three products: TBF-A−NAC monoadduct, *m*/*z* 300 (70% relative intensity, TBF-A−NAC + 1) and 317 (100% relative intensity, TBF-A−NAC + 1 + NH_3), with a t_R of 20 min; and TBF-A−diNAC diastereomers, *m*/*z* 463 (100% relative intensity, TBF-A−diNAC + 1) with t_Rs of 17.4 and 18.3 min. The positive ion LC/MS/MS spectrum of the monoadduct (t_R = 20 min) consisted of fragments with *m*/*z* 300 (10% relative intensity, TBF-A−NAC + 1, unfragmented) and *m*/*z* 137 (100% relative intensity, TBF-A^+). The fragments of the diadducts (t_R = 17.4 and 18.3 min) were *m*/*z* 463 (50% relative intensity, TBF-A−diNAC + 1, unfragmented), 342 (30% relative intensity), 300 (15% relative intensity, TBF-A−NAC), and 137 (100% relative intensity, TBF-A).

Exchange of thiol groups was investigated by adding 134 mg of reduced GSH (5 mM final concentration) to the above solution of TBF-A−NAC conjugates at pH 7.38. The reaction between TBF-A and NAC was followed by HPLC to ensure that all the TBF-A was consumed prior to the addition of GSH. The mixture was incubated at 37 °C for 6 h, and the crude reaction mixture was analyzed immediately by LC/MS using standard HPLC conditions. For MS/MS analyses, buffer salts were removed by solid-phase extraction as described above (10% acetonitrile as eluent) and then concentrated by vacuum. LC/MS was performed in the positive ion mode, and all peaks were quantified using the TBF-A−NAC signal as the reference (100%). The relative ion currents of the ions were as follows: *m*/*z* 300 (100% relative intensity, TBF-A−NAC), t_R = 19.8 min; *m*/*z* 463 (33.4% relative intensity, TBF-A−diNAC), t_R = 17.3 and 18.3 min; *m*/*z* 444 (10.8% relative intensity, TBF-A−GSH), t_R = 15.5 and 17.2 min; *m*/*z* 607 (10.6% relative intensity, TBF-A−NAC−GSH), t_R = 15.2 and 16.0 min; and *m*/*z* 767 (4.4% relative intensity, TBF-A−diGSH + NH_3), t_R = 16.0, 16.2, 16.4, and 16.8 min. The MS/MS spectrum of the GSH monoadducts consisted of peaks with *m*/*z* 444 (30% relative intensity, TBF-A−GSH), 230 (90% relative intensity), and 137 (100% relative intensity, TBF-A^+). The MS/MS spectrum of the GSH diadducts consisted of peaks with *m*/*z* 767 (40% relative intensity, TBF-A−diGSH + NH_3), 460 (100% relative intensity, TBF-A−GSH^+), and *m*/*z* 189 (20% relative intensity). The MS/MS spectrum of the NAC and GSH diadduct consisted of peaks with *m*/*z* 607 (90% relative intensity, TBF-A−NAC−GSH) and 137 (30% relative intensity, TBF-A^+).

Preparation of Microsomes. Microsomes were prepared from fresh female rat liver (Lewis, Charles River, 300 g), and the protein and P450 concentrations were determined. Briefly, whole female rat livers (two) were washed with cold sucrose buffer (0.25 M) and then weighed. The livers were transferred to a homogenizer tube, diluted 4-fold with sucrose buffer, and then minced with scissors prior to homogenization. The liver pieces were homogenized using an electric homogenizer until no chunks of liver remained. The homogenate was then centrifuged at 10000*g* for 25 min (4 °C). The pellet portion was resuspended in cold sucrose buffer and centrifuged at 10000*g* for 25 min. The supernatant from the second centrifugation was added to that from the first and centrifuged at 100000*g* (4 °C) for 90 min. The microsomal pellet was resuspended in cold storage buffer (100 mM phosphate, 1 mM EDTA, and 10% glycerol). The protein concentration was determined using the modified Lowry method (albumin standards), and the P450 concentration was determined by reducing the microsomes with sodium dithionite and bubbling a stream of carbon monoxide through the solution to form a $[Fe(CO)]^{2+}$ complex. This solution was then analyzed by difference UV spectroscopy, and the P450 concentration was determined using the extinction coefficient difference between 450 and 490 nm [$\Delta\epsilon_{heme}$(CO compound − reduced compound) = 91 cm^{-1} mM^{-1}] (*15*).

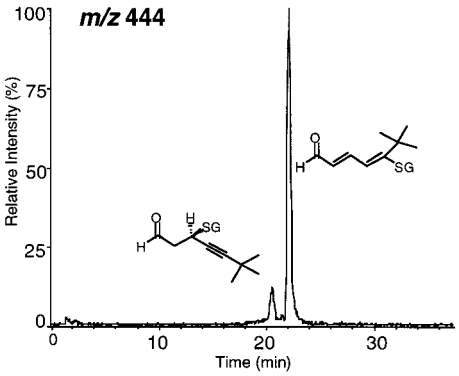

Figure 2. LC/MS (*m*/*z* 444, extracted) profile of synthetically generated TBF-A−GSH conjugates. The conjugate was synthesized by adding purified TBF-A (0.2 mM final concentration) to 10 mM GSH in 100 mM phosphate buffer (pH 8.0).

Microsomal Incubations. Rat and human liver microsomal incubations contained 2 mg (0.87 of nmol P450/mL) and 14 mg of microsomal protein, respectively. Incubations were conducted for 1 h at 37 °C in 100 mM phosphate buffer (pH 7.4, 1 mL total volume). A terbinafine stock solution (100 mM in 75% acetonitrile in water) and GSH were added in phosphate buffer (pH 7.4) to achieve final concentrations of 0.4 and 1 mM, respectively. The final incubations contained 0.3% (v/v) acetonitrile. The NADPH-generating system consisted of 0.4 mM $NADP^+$, 7.5 mM glucose 6-phosphate, 1.25 unit/mL glucose-6-phosphate dehydrogenase, and 5.0 mM magnesium chloride.

The assay described above for determining the P450 concentration in human liver microsomes was not successful due to the concentration of P450 being approximately 10-fold lower than in rat liver microsomes; instead, an assay based on the metabolism of *p*-nitrophenol was used to determine P450 activity of human microsomes. For negative control incubations, either $NADP^+$ was omitted or the microsomal incubation was boiled for 3 min. The reactions were initiated by the addition of $NADP^+$ and terminated by chilling in an ice bath followed by the addition of ice-cold acetonitrile (2 mL). Aliquots were analyzed by LC/MS as described in the analytical section.

Results

The synthetic generation of TBF-A−GSH adducts (TBF-A−SG) yielded two monoadducts and a trace of the diadduct. Figure 2 shows the LC/MS trace of the crude TBF-A−SG monoadducts, which both have ions at *m*/*z* 444 and t_Rs of 20.5 and 22.0 min. A trace of diadduct (*m*/*z* 767, M + 2GSH + H^+ + NH_3) was seen at 16 min of this run (not seen in Figure 2 due to ion extraction). LC/MS/MS of the 22 min peak showed the loss of GS^-, leaving a fragment of *m*/*z* 137 (100% relative intensity) that corresponds to protonated TBF-A (data not shown but analogous to Figure 6).

The anticipated product of N-dealkylation of terbinafine was synthesized in an effort to characterize its GSH conjugates. The synthesized TBF-A was an *E*/*Z* mixture and was determined to be 85% *E* by ^{1}H NMR (Figure 3A).

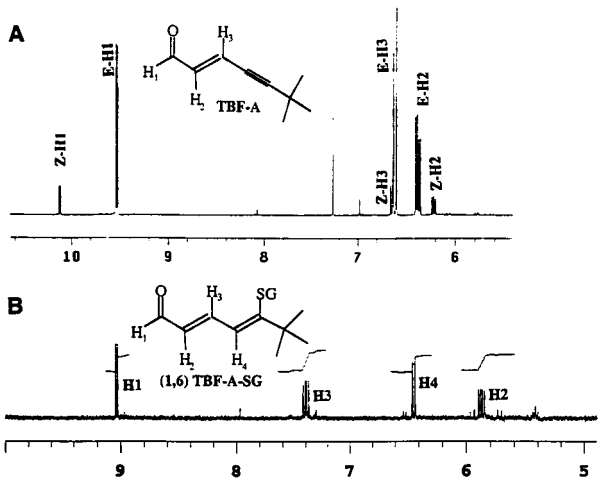

Figure 3. ^{1}H NMR spectra of the purified 1,6-TBF-A−SG adduct (B) and the starting material, TBF-A (A). Chemical shifts were assigned using (A) $CDCl_3$ (δ 7.24) and (B) D_2O (δ 4.63, unsuppressed) as reference peaks.

The two protons (H2 and H3) of the major isomer were trans to one another as shown by the larger coupling constants (J = 16 Hz) of the major H2 and H3 peaks (δ 6.38 and 6.61 ppm, respectively) compared to the smaller coupling constants of the corresponding minor peaks. Upon isolation of the GSH adducts, the ^{1}H NMR spectrum (Figure 3B) exhibited four peaks in the downfield region of the spectrum in addition to peaks characteristic of GSH in the upfield region. The three downfield peaks between δ 5.90 and 7.40 ppm represented the three "allene" protons that arose when GSH was added in a 1,6-Michael fashion to TBF-A. If the addition had occurred via a 1,4-addition, we would expect only two peaks in this region because aliphatic hydrogens are generated by this mechanism. The doublet at 9.05 ppm represents the aldehyde proton (H1); therefore, the predominant GSH adduct is the (*E*)-1,6-TBF-A−SG adduct.

The identity of the minor adduct was demonstrated indirectly by HPLC with UV/vis detection to be the 1,4-GSH adduct. The minor *m*/*z* 444 peak shown in Figure 2 was not detected by the UV detector at 270 nm, thus confirming the loss of the chromophore. Another possible monoadduct could arise from a 1,6-GSH addition to the less abundant *Z* isomer of TBF-A. However, if the latter corresponded to the 20 min peak, it should be detectable due to absorption at 270 nm. Thus, due to its lack of UV absorption coupled with its mass, the minor adduct shown in Figure 2 must be the 1,4-TBF-A−SG adduct.

NAC adducts of TBF-A were synthesized and purified in an effort to investigate whether the Michael addition of thiol nucleophiles is reversible. After incubation of GSH with the mono- and di-NAC adducts of TBF-A, LC/MS and MS/MS data demonstrated the presence of four di-GSH adducts in addition to the two mono-GSH adducts previously identified (Figure 4). Qualitative analysis of the adduct signals before and after addition of GSH showed decreasing levels of mono- and di-NAC adducts with introduction of signals corresponding to GSH adducts. If it is assumed that all NAC and GSH conjugates of TBF-A have similar ionization efficiencies, mass balance analysis (Figure 4) showed 99% recovery of signal after GSH addition, indicating that the observed GSH adducts indeed arose from the corresponding NAC adducts. Thus, the reaction of TBF-A with thiol nucleophiles appears to be reversible.

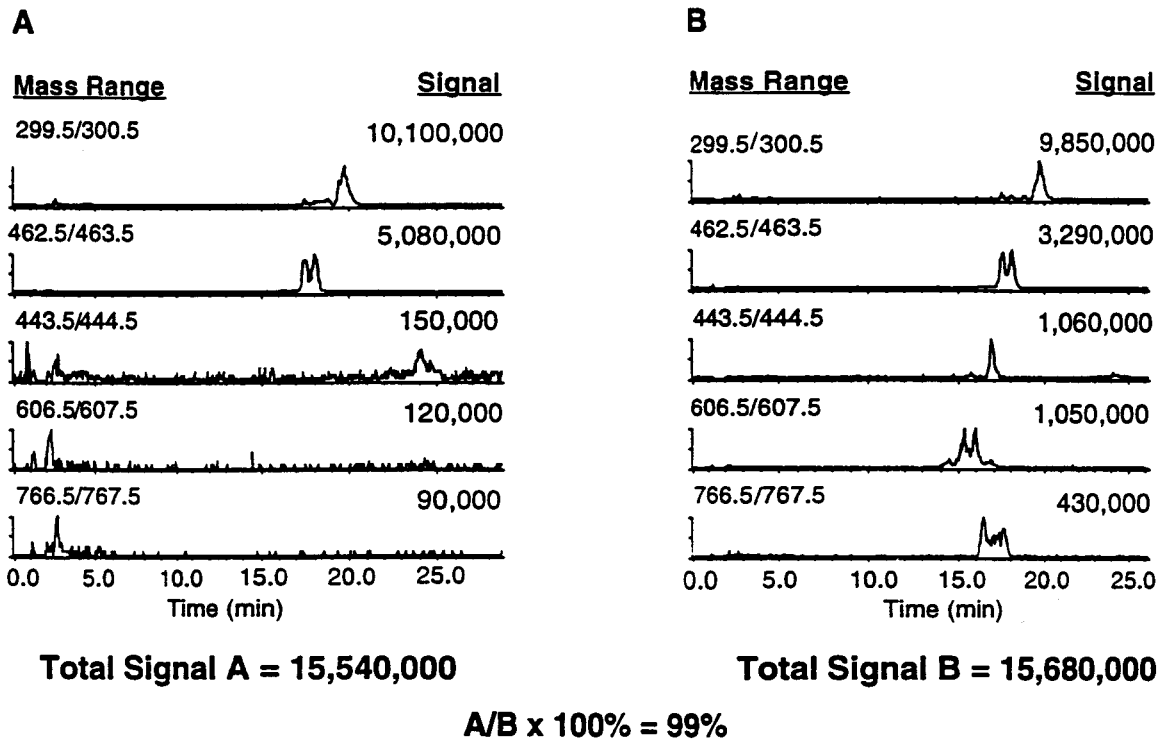

Figure 4. Reversibility of thiol addition to TBF-A. Each chromatogram shows one ion that was extracted from the LC/MS data of (A) NAC adducts after reaction of TBF-A (0.43 mM) with NAC (15 mM, pH 8.0) and (B) NAC and GSH adducts after addition of GSH (5 mM) to the reaction mixture described above (final pH of 7.38). The mass ranges (left side of diagrams) are representative of the following molecular ions: 300 (TBF-A−NAC), 463 (TBF-A−diNAC), 444 (TBF-A−GSH), 607 (TBF-A−NAC−GSH), and 767 (TBF-A−diGSH). The mass balance calculation was carried out using the equation Σ(signals in analysis A)/Σ(signals in analysis B) × 100% (assuming similar ionization energies of both NAC and GSH conjugates of TBF-A).

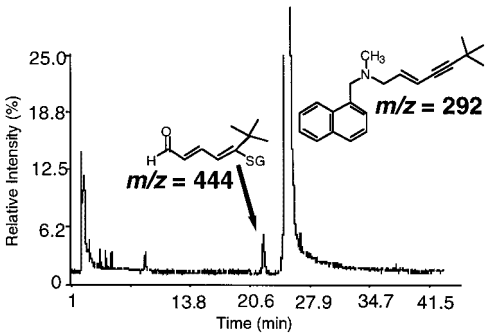

Figure 5. LC/MS profile of the deproteinized rat liver microsomal incubation with terbinafine. The detector was programmed to selectively detect species with *m*/*z* 292 (terbinafine + 1) and *m*/*z* 444 (TBF-A−SG) (selective ion monitoring). Incubations containing 0.87 nmol of P450/mL were conducted for 1 h at 37 °C in 100 mM phosphate buffer (pH 7.4, 1 mL total volume). Terbinafine was added as a solution in 75% acetonitrile and GSH in phosphate buffer to achieve final concentrations of 0.4 and 1 mM, respectively. The GSH conjugate had a retention time identical to that of its synthesized counterpart.

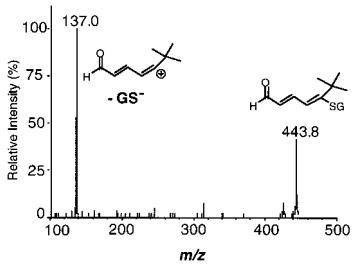

Figure 6. LC/MS/MS of the 1,6-GSH conjugate (1,6-TBF-A−SG, 22 min peak). The conjugate was generated by incubation of terbinafine with the rat liver microsomal protein in the presence of GSH. The fragmentation pattern was identical to that of the synthesized 1,6-GSH conjugate.

The rat and human microsomal incubations with terbinafine yielded the same TBF-A−GSH monoadducts that were seen in the synthetic experiments (Figures 5−7). The LC/MS analyses of the rat microsomal incubations involved using SIM. In this case (Figure 5), the computer looked for ions at *m*/*z* 292 (terbinafine) and 444 (TBF-A−SG + H). Therefore, if other ions were present, they would not be detected in this spectrum. Extraction of the *m*/*z* 444 signals from the data shown in Figure 5 revealed peaks at 20.5 and 22 min (extraction trace not shown). The 22 min peak corresponding to the 1,6-TBF-A−SG adduct can be seen in Figure 5. To gain further proof that the 1,6-TBF-A−SG adduct was the major GSH adduct formed during the rat microsomal incubation, the sample was injected again and MS/MS data were obtained for the 22 min species (Figure 6). The fragment pattern was the same as that for the synthetic 1,6-GSH adduct (data not shown).

We wanted to merely demonstrate that there were active P450s present in the human liver microsomes as shown by the oxidation of *p*-nitrophenol to the corresponding catechol (data not shown). Greater sensitivity was required for the analyses of the human microsomal incubations with terbinafine, which involved setting the mass spectrometer in MRM mode (see Materials and Methods) and disconnecting the column from the mass spectrometer interface until data collection was necessary (to avoid contamination of the interface with buffer salts and protein). Data collection commenced 18 min postinjection; thus, the TBF-A−SG adduct and terbinafine exhibited retention times of 4 and 6 min, respectively (Figure 7A). Analyses of the incubates (Figure 7A) showed the presence of a TBF-A−SG species with a protonated ion at *m*/*z* 444, a major fragment ion at *m*/*z* 137, and a retention time of 22 min (data not collected for first 18 min). The GSH conjugate of TBF-A was absent from the control incubation (Figure 7B). Hence, both rat and human P450 enzymes catalyzed the N-dealkylation reaction of terbinafine to yield TBF-A, which in turn reacted with thiol nucleophiles.

Discussion

The usual time between the start of terbinafine treatment and the onset of clinical signs of cholestatic hepatitis is 2−4 weeks. Seven reported case studies indicate that the initial symptoms include weakness, fatigue, dark urine, pale stools, and/or jaundice (*3*, *16*−*21*). Liver biopsies of affected patients usually revealed intact liver architecture with hepatocyte degeneration and canalicular cholestasis leading to bile stasis (brown pigment) and bile thrombus formation (*16*−*18*). More severe cases revealed bile duct necrosis with eosinophil accumulation in the portal tracts (*17*), while one case showed a nearly complete disappearance of hepatocytes (*19*). Less severe cases did not involve necrosis and/or mononuclear cell migration (*3*).

Although terbinafine-induced cholestasis appears to be reversible upon terbinafine withdrawal, two case reports indicated persistent cholestasis (>6 months) (*17*, *21*), while one case report described fulminant hepatic failure requiring transplantation (*19*). Fernandes et al. reported persistent asymptomatic, abnormally high levels of alkaline phosphatase, aminotransferases, and γ-glutamyl transferase. Mallat et al. provided the only case to date that had characteristics of "vanishing duct syndrome", i.e., a permanent reduction in the number of interlobular bile ducts (*21*). Likewise, earlier reports of histologically documented cholangitis suggest that interlobular bile ducts are the targets in terbinafine-induced liver injury (*16*, *18*).

The literature presents little discussion concerning the possible mechanism(s) of terbinafine-induced hepatitis. Due to the idiosyncratic nature of this adverse drug reaction, most attribute the mechanism to "an uncommon immunological and/or metabolically mediated effect" (*3*, *18*, *22*). The few in vivo models of cholestasis suggest that the pathogenesis of drug-related biliary damage involves covalent modification of liver cell peptides by reactive metabolites of the drug (*22*). Clinical studies provide strong evidence that the pathogenesis of halothane-induced hepatitis involves an immune-mediated mechanism (i.e., eosinophilia and circulating antibodies to P450) where the reactive metabolite of halothane conjugates with liver cell proteins that act as immune targets (*23*). Eosinophil accumulation was seen in at least one case of terbinafine-induced hepatitis, whereas neutrophil accumulation, the hallmark of the α-naphthylisothiocyanate (ANIT) model for cholangiolitis, was absent from all documented terbinafine-induced hepatitis cases. Neutrophil infiltration was not reported in the single case of terbinafine-induced cholangitis (*21*).

As in the halothane model, the protein-modifying capacity of ANIT is presumed to be the cause of the immune response, however, via a different mechanism from that proposed for halothane. It appears that the mechanism involves the following steps. ANIT is trans-

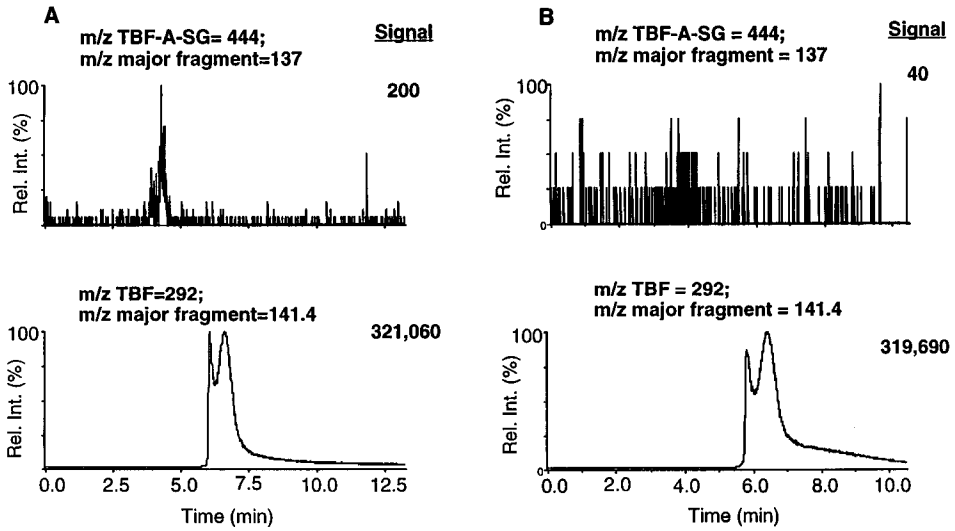

Figure 7. LC/MS/MS profiles of the deproteinized human liver microsomal incubation with terbinafine (A) and the control incubation (B, boiled enzyme). The detector was programmed to identify species with a specific *m/z* corresponding to its unique MS/MS fragment (multiple-reaction monitoring). The bottom chromatograms show the parent compound, terbinafine, was present in both incubations, whereas the top chromatograms show either the presence (A) or absence (B) of the TBF-A−SG adduct. Data collection commenced 18 min postinjection. The GSH adduct had a retention time identical to that of the synthesized 1,6-GSH conjugate. Incubations containing 14 mg of protein were conducted for 1 h at 37 °C in 100 mM phosphate buffer (pH 7.4, 1 mL total volume). Terbinafine was added as a solution in 75% acetonitrile (acetonitrile was 0.3% of the total incubation volume) and GSH in phosphate buffer to achieve final concentrations of 0.4 and 1 mM, respectively.

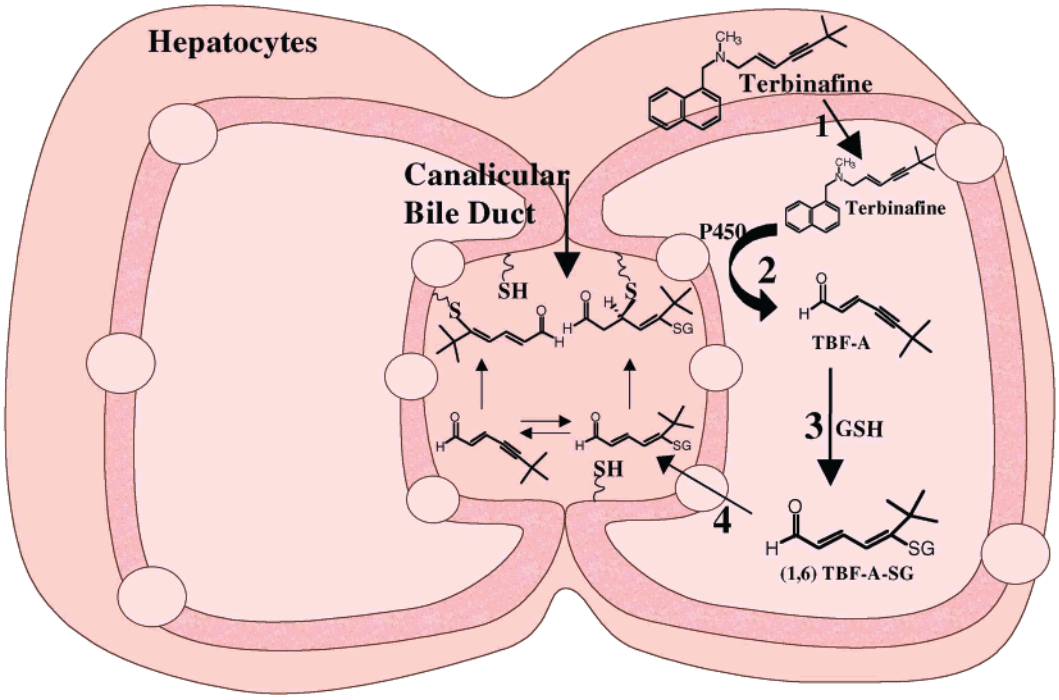

Figure 8. Hypothesis of terbinafine-induced cholestatic hepatitis. (1**)** Terbinafine translocation across the hepatocyte membrane. (2) P450-catalyzed N-dealkylation to form TBF-A. (3) Conjugation of TBF-A with GSH to form the 1,6-TBF-A−SG adduct. (4) Transport of the TBF-A−SG adduct across the canalicular membrane where it is concentrated and can conjugate with thiol groups of canalicular proteins.

ported across the canalicular membrane as its GSH conjugate, and it is concentrated in the bile. There, the reverse reaction occurs, yielding concentrated amounts of ANIT, which then interacts with bile duct epithelial cells. These modified cells produce "factors" that attract proteolytic enzyme-releasing neutrophils which, recognizing the modified bile duct epithelial cell as "foreign", destroy the ductule cells leading to obstruction of bile flow.

In line with the early pathogenic features of the halothane, ANIT, and other models of cholestatic hepatitis, we postulated the formation of a reactive metabolite of terbinafine in the liver capable of covalently binding to proteins and concentrating in the bile. Indeed, high concentrations of terbinafine are found in the liver after parental administration (*12*, *24*), and the drug is extensively metabolized by P450s (*25*). A recently published study revealed that at least seven P450 enzymes are involved in terbinafine metabolism with P450s 2C9, 2C8, 1A2, and 3A4 being implicated in dealkylation reactions (*26*). In this study, we unveiled a reactive metabolite, TBF-A, generated from incubations with both rat and

human liver microsomal protein. This type of unsaturated aldehyde is a good Michael acceptor, and reacted with GSH by either a 1,4- or 1,6-addition to form the adducts shown in Figure 2. We speculate (Figure 8) that TBF-A is formed by liver enzymes, conjugated with GSH, transported across the canalicular membrane of hepatocytes, and concentrated in the bile. The major GSH adduct is the 1,6-addition product, which is still reactive and can bind to hepatobiliary proteins. These steps are reminiscent of those described above in the ANIT model of cholestatic hepatitis. Yet, TBF-A could be even more efficient at modifying canalicular protein because it is still electrophilic as a monoadduct, as well as after GSH dissociation. We propose that TBF-A is responsible for the hepatic dysfunction that is observed among patients treated with terbinafine.

References

(1) Gupta, A. K., and Shear, N. H. (1997) Terbinafine: An update. *J. Am. Acad. Dermatol.* **37**, 979−988.

(2) Abdel-Rahman, S. M., and Nahata, M. C. (1997) Oral Terbinafine: A New Antifungal Agent. *Ann. Pharmacother.* **31**, 445−456.

(3) Gupta, A. K., Del Rosso, J. Q., Lynde, C. W., Brown, G. H., and Shear, N. H. (1998) Hepatitis associated with terbinafine therapy: three case reports and a review of the literature. *Clin. Exp. Dermatol.* **23**, 64−67.

(4) Gupta, A. K., Kopstein, J. B., and Shear, N. H. (1997) Hypersensitivity reaction to terbinafine. *J. Am. Acad. Dermatol.* **36** (6, Part 1), 1018−1019.

(5) Amichai, B., and Grunwald, M. H. (1998) Adverse drug reactions of the new oral antifungal agents: terbinafine, fluconazole, and itraconazole. *Int. J. Dermatol.* **37**, 410−415.

(6) Hall, M., Monka, C., Krupp, P., and O'Sullivan, D. (1997) Safety of oral terbinafine: Results of a postmarketing surveillance study in 25884 patients. *Arch. Dermatol.* **133**, 1213−1219.

(7) Terbinafine Product Monograph, Canada (1995) pp 1−33, Dorval, QC, Sandoz, Canada.

(8) Erlinger, S. (1997) Drug-induced cholestasis. *J. Hepatol.* **26** (Suppl. 1), 1−4.

(9) Kenna, G. J. (1997) Immunoallergic drug-induced hepatitis: Lessons from halothane. *J. Hepatol.* **26** (Suppl. 1), 5−12.

(10) Kossor, D. C., Meunier, P. C., Dulik, D. M., Leonard, T. B., and Goldstein, R. S. (1998) Bile duct obstruction is not a prerequisite for type I biliary epithelial cell hyperplasia. *Toxicol. Appl. Pharmacol.* **152** (2), 327−338.

(11) Battig, F. A., Nefzger, M., and Schulz, G. (1987) in *Major biotransformation routes of some allylamine antimycotics*, pp 479−495, J. R. Prous Science Publishers, S. A., Barcelona, Spain.

(12) Jensen, J. C. (1989) Clinical pharmacokinetics of terbinafine (Lamisil). *Clin. Exp. Dermatol.* **14**, 110−113.

(13) Humbert, H., Denouel, J., Cabiac, H., and Sioufi, A. (1998) Pharmacokinetics of terbinafine and five known metabolites in children, after oral administration. *Biopharm. Drug Dispos.* **19**, 417−423.

(14) Kaminsky, L. S. (1985) Benzene and Substituted Benzenes. In *Bioactivation of Foreign Compounds* (Anders, M. W., Ed.) pp 157−170, Academic Press, Orlando, FL.

(15) Omura, T., and Sato, R. (1964) The carbon monoxide-binding pigment of liver microsomes. I. Evidence for its hemoprotein nature. *J. Biol. Chem.* **239**, 2370−2378.

(16) Lazaros, G. A., Papatheodoridis, G. V., Delladetsima, J. K., and Tassopoulos, N. C. (1996) Terbinafine-induced cholestatic liver disease. *J. Hepatol.* **24**, 753−756.

(17) Fernandes, N. F., Geller, S. A., and Fong, T.-L. (1998) Terbinafine Hepatotoxicity: Case report and review of the literature. *Am. J. Gastroenterol.* **93** (3), 459−460.

(18) van't Wout, J. W., Hermann, W. A., de Vries, R. A., and Stricker, B. H. (1994) Terbinafine associated hepatic injury. *J. Hepatol.* **21**, 115−117.

(19) Agarwal, K., Manas, D. M., and Hudson, M. (1999) Terbinafine and fulminant hepatic failure. *N. Engl. J. Med.* **340** (16), 1292−1293.

(20) Dwyer, C. M., White, M. I., and Sinclair, T. S. (1997) Cholestatic jaundice due to terbinafine. *Br. J. Dermatol.* **136**, 976−977.

(21) Mallat, A., Zafrani, E. S., Metreau, J. M., and Dhumeaux, D. (1997) Terbinafine-induced prolonged cholestasis with reduction of interlobular bile ducts. *Dig. Dis. Sci.* **42** (7), 1486−1488.

(22) Geubel, A. P. (1998) Drug-related biliary damage: A peculiar condition involving a genetic predisposition? *Acta Gastro-Enterol. Belg.* **61**, 2−3.

(23) Kenna, J. G., and van Pelt, F. N. A. M. (1994) The metabolism and toxicity of inhaled anaesthetic agents. *Anaesth. Pharmacol. Rev.* **2**, 29−42.

(24) Balfour, J. A., and Faulds, D. (1992) Terbinafine. A review of its pharmacodynamic and pharmacokinetic properties, and therapeutic potential in superficial mycoses. *Drugs* **43**, 259−284.

(25) Trepanier, E. F., Nafziger, A. N., Kearns, G. L., Kashuba, A. D. M., and Amsden, G. W. (1998) Absence of effect of terbinafine on the activity of CYP1A2, NAT-2 and xanthine oxidase. *J. Clin. Pharmacol.* **38**, 424−428.

(26) Vickers, A. E., Sinclair, J. R., Zollinger, M., Heitz, F., Glanzel, U., Johanson, L., and Fischer, V. (1999) Multiple cytochrome P-450s involved in the metabolism of terbinafine suggest a limited potential for drug-drug interactions. *Drug Metab. Dispos.* **27** (9), 1029−1038.

TX0002029